Eur. Phys. J. A (2024) 60:248
https://doi.org/10.1140/epja/s10050-024-01451-y

THE EUROPEAN PHYSICAL JOURNAL A

Regular Article - Theoretical Physics

Random files for fission fragment evaporation in TALYS: a total Monte Carlo approach

P. Karlsson[1], A. Al-Adili[1,a], A. Göök[1], Z. Gao[1], S. Pomp[1], H. Sjöstrand[1], A. Solders[1], A. Koning[2]

[1] Department of Physics and Astronomy, Uppsala University, 751 20 Uppsala, Sweden
[2] NAPC-Nuclear Data Section, International Atomic Energy Agency, Vienna International Centre, 1400 Vienna, Austria

Received: 23 August 2024 / Accepted: 9 November 2024

Communicated by Cedric Simenel

Abstract In this study, we have applied the Total Monte Carlo (TMC) methodology in the simulation of the de-excitation process of primary fission fragments (FF) within the TALYS code. Our objective was to develop a method for assessing fission model deficiencies and parameter sensitivities. The input fission fragment data used by TALYS were systematically varied. This was done using the GEF code to generate 10,000 random files by randomizing the 94 model parameters of GEF that influence both fission yields and their energy distributions. The GEF parameters were varied randomly within 3% of the default value, assuming a normal probability distribution. As a result of this parameter variation, significant changes could be identified for several observables, including the multiplicities of γ rays and prompt neutrons, as well as their spectra. Additionally, we investigate the impact of angular momentum distribution on the de-excitation data of both GEF and TALYS. Finally, we present an attempt to construct a best parameter file benchmarked against evaluated nuclear data files.

1 Introduction

In nuclear fission, highly excited fission fragments (FF) are formed. The nuclear de-excitation process gives rise to evaporated prompt particles, such as neutrons and γ rays. Nuclear data from the fission evaporation mechanisms play a crucial role in both nuclear technology and the theoretical modeling of nuclear fission. Essential to this field of study are correlated fission data, which encompass a variety of key parameters. These include, but are not limited to, the independent yields of fission products, the neutron and gamma multiplicities, and the energy spectra of prompt fission neutrons, γ-rays, and isomeric yield ratios.

The modeling of these observables is inherently complex, particularly when different fission systems and excitation energies are taken into account. Contemporary efforts in fission modeling are directed towards describing and predicting the correlations within fission data, especially in contexts where empirical data are absent. It has been a rather challenging task to accurately describe the multiplicities and energies of neutrons and γ-rays simultaneously [1]. In an attempt to address this problem, a new feature was recently implemented in the TALYS reaction code, as reported by Fujio et al. [2,3]. This feature enables TALYS to simulate a full nuclear de-excitation of a predefined list of nuclides produced in fission, and to calculate relevant evaporation data for the selected fission reaction. The predefined format for a list of nuclides allows all users to create custom-made databases to feed into TALYS. This functionality facilitates direct comparisons between calculated evaporation data and experimental observations, which are essential for benchmarking modeled mass yields, excitation energy sharing, and angular momentum generation. The underlying theoretical framework for this work builds on the Hauser-Feshbach formalism [4]. Fission theorists have the option of providing standardized tables with modeled primary fission data. The use of the sophisticated de-excitation and evaporation methodology of TALYS commonly provides the ability to better assess possible fission model defects.

As a proof of principle, in an earlier study, the GEF code [5] was employed to produce 737 databases for different compound nuclei and excitation energies [6]. The databases were benchmarked for several reactions, most notably for the thermal fission of ^{235}U(n,f) [2]. The evaluation revealed a generally satisfactory performance. However, it also brought to light certain discrepancies, particularly in the prompt fission neutron spectrum, and in the multiplicities and energies associated with γ-ray emissions.

[a] e-mail: ali.al-adili@physics.uu.se (corresponding author)

Published online: 19 December 2024

In the proof-of-principle study, a limited sensitivity study was conducted in Ref. [2] to investigate the impact of TALYS parameter adjustment on the evaporation data. These parameters control e.g. the excitation energy binning of the fission fragments and subsequent decay products, the angular momentum population in the nascent fragments, and the spin cut-off parameter of the nuclear level densities. However, the study did not alter certain key initial conditions of the primary fission fragments, such as the fission yields and their excitation energies. This fact raises an important question: how do uncertainties and potential model defects, in determining fission yields and excitation energy distributions, influence the evaporation observables (such as multiplicities and spectra of prompt and delayed particles) from fission? To explore this question, our current study introduces random perturbations to the fission model parameters within the GEF framework to create varied input files. These are then fed into the TALYS code to generate random databases. Although a proper sensitivity analysis is beyond the scope of this work, we present the methodology and a proof-of-principle case for the implementation of a Total Monte Carlo (TMC) method to quantify the sensitivities of the de-excitation results to such perturbations.

In the following section of this paper, we review the essential input data required to conduct calculations using the TALYS code. This includes a description of the necessary input databases. Section 4 presents an overview of the methodologies employed, including the application of the TMC methodology within our study's framework. Finally, Sect. 5 contains results obtained from the TALYS calculations using perturbed input data from GEF, in comparison with the default results. The paper concludes with an outline for the future progress needed to further develop the methodology.

2 Background

In a fission event, the Q-value denotes the difference between the masses before and after scission, including the energy brought by the incident particle. The Q-value, including the excitation energy of the compound nucleus, is shared between the total excitation energy (TXE) and the total kinetic energy (TKE):

$$Q = \mathrm{TKE} + \mathrm{TXE}. \tag{1}$$

On average, TKE constitutes approximately 80–90% of the Q value, though this proportion can vary significantly from one fission event to another. The TXE is primarily made up of three components: intrinsic energy, collective energy, and deformation energy. It is generally accepted that, immediately after the shape relaxation, the deformation energy transforms into intrinsic excitation energy. Therefore, at the point of full acceleration, a fission fragment i typically possesses a TXE that is composed of rotational energy ($E_{i,\mathrm{rot}}$), owed to the collective motion, and intrinsic energy (E_i^*) [7]:

$$\mathrm{TXE} = E_1^* + E_{1,\mathrm{rot}} + E_2^* + E_{2,\mathrm{rot}}, \tag{2}$$

where the rotational energy is a function of the total angular momentum (J) and the moment of inertia ($\mathcal{I}$):

$$E_{\mathrm{rot}} = \frac{\hbar^2}{2\mathcal{I}} J\,(J+1)\,. \tag{3}$$

The sharing of the total excitation energy between the FFs and the angular momentum generation are still unsolved problems in contemporary fission theory [8–13]. In order to properly assess the theoretical modeling of energy and angular momentum sharing, one needs to evaluate the full correlation of fission de-excitation data, considering the multiplicities and spectra of both prompt and delayed particles.

TALYS assumes a Gaussian excitation energy distribution for fission fragments with the same A and Z. Each distribution is characterized by a mean energy, $\bar{E}^*$, and an energy spread, σ_{E^*}. The angular momentum, on the other hand, is widely modeled based on the so-called Rayleigh distribution, as adopted from the level density formalism [14].

3 Input to TALYS

When conducting fission fragment calculations using TALYS, input data for the fission fragments can be taken from one of several internal databases. These databases supply TALYS with the following information:

- independent fission fragment yields $Y_{\mathrm{ff}}(Z, A)$
- the mean excitation energy $\bar{E}^*$ and the width σ_{E^*} of the excitation energy distribution for each fragment species (same A and Z)
- average total kinetic energy ($\overline{\mathrm{TKE}}$) and total excitation energy ($\overline{\mathrm{TXE}}$) for each fragment pair.

From the associated Gaussian excitation energy distribution, TALYS models the evaporation process, e.g., neutron and γ-ray emissions, until both fragments reach their ground states or isomeric states. The kinetic energies are necessary to convert the neutron energy spectrum from the center of mass of the emitting fragment frame to the laboratory frame, following Feather's method [17].

GEF is a Monte Carlo-based phenomenological fission model which can generate data on various quantities, both pre and post-neutron emission. Furthermore, it simulates fragment de-excitation by employing a simplified evaporation

scheme. In a previous work, GEF (version: 2021/1.2) was employed to produce the mass and charge yields of primary fission fragments and their corresponding energies [6]. Nordström sampled 1 million Monte Carlo fission events for each of 737 fissioning nuclei, ranging from $_{76}$Os to $_{115}$Mc, at excitation energies ranging from 0 to 20 MeV. The list-mode data feature was activated to allow for an event-by-event output of each fission simulation. The generated GEF data ($Y_{\mathrm{ff}}(Z, A)$, $\bar{E}^*$, σ_{E^*}, $\overline{\mathrm{TKE}}$) was stored, in a tabulated format, in the TALYS fission fragment database. TALYS gives the option to use the GEF data listed in the database for the de-excitation process (among other fission models), constructing the excitation energy distribution from the provided mean energies $\bar{E}^*$ and widths σ_{E^*}, assuming a Gaussian distribution:

$$G(E^*) = \frac{1}{\sqrt{2\pi}\sigma_{\mathrm{E}^*}} \exp\left\{-\frac{(E^* - \bar{E}^*)^2}{2\sigma_{\mathrm{E}^*}^2}\right\}. \tag{4}$$

Another important aspect in addition to the excitation energy is the angular momentum population. TALYS adopts a spin-parity distribution $R(J, \pi, E^*)$ following the functional dependency of the level density formalism [18]:

$$R(J, \pi, E^*) = \frac{1}{2} \cdot \frac{2J+1}{2f^2\sigma^2(E^*)} \exp\left\{-\frac{(J+\frac{1}{2})^2}{2f^2\sigma^2(E^*)}\right\}, \tag{5}$$

where f acts as a scaling factor governing the angular momentum in the primary fission fragments [19]. TALYS enables the adjustment of the overall angular momentum population in the fission fragments through the use of the *Rspincutff* keyword, which modifies the scaling parameter f. In a similar manner, there is another scaling factor, f_{s}, which represents a global adjustment factor of the nuclear spin cut-off parameter, applicable for the level density model. The f_{s} scaling parameter affects all nuclei which are populated after the onset of the primary fission fragment evaporation. In TALYS, the f_{s} parameter can be modified using the *Rspincut* keyword, and has a default value of 1.0. Recent independent research indicates that the spin cut-off parameter has typically been overestimated, and should instead be around 0.4–0.5 [2,20,21].

4 Methodology

4.1 Total Monte Carlo

The uncertainties of simulation results are commonly calculated through the combined use of sensitivity analysis, perturbation theory, and co-variance matrices [22]. Large-scale error propagation and perturbation analysis can sometimes be cumbersome when applied on large models with many compensating parameters. Sometimes this even leads to inaccurate uncertainty propagation, especially when applied to non-linear models. A way to mitigate this issue is by implementing the Total Monte Carlo method [22]. The TMC method has been successfully employed in a number of applications [23]. It is especially suitable for calculations involving numerous parameter combinations and permutations [24]. One such case is the GEF fission model, which has 94 model parameters. These parameters are correlated, and by using the TMC method, these correlations can implicitly be accounted for [22]. The results of a TMC simulation contains two sources of uncertainties, a statistical uncertainty (due to the Monte Carlo simulations) and a systematical uncertainty (due to the model assumptions) [22]. Central to the idea of the TMC method is the automation of the calculation process with the introduction of as little bias as possible at the intermediate steps [25]. As an adaption of the TMC method, the GEF and TALYS codes were coupled [26]. Perturbed fission fragment data from GEF were used as input data for the calculation of the evaporation process by a Hauser-Feshbach model in TALYS [23]. The perturbed data were produced by adding random perturbations to the default values of the GEF fission parameters. This was done using the built-in function *MyParameters*, which allows simulations to be made with individually chosen parameter values [27]. The default function does not include all parameters, and hence the function was modified and extended to include all 94 parameters [26]. The perturbed parameter values were drawn from a normal distribution centered on the default parameter value, with the standard deviation set to 3% of the default parameter value. Higher levels of parameter variation were avoided in order to remain within the numerical stability range of GEF. The independent parameter variation of each fission mode (standard-1, standard-2, and super-long) was performed, considering the relative mode weights and normalizing the fission yields to 200%. For parameters with a default value of zero, the standard deviation was set to 0.03. Following the procedure described in Sect. 3, 10,000 perturbed sets of data for $\mathrm{Y_{ff}}(Z,A)$, $\overline{E^*}$, σ_{E}^*, $\overline{\mathrm{TXE}}$, and $\overline{\mathrm{TKE}}$ were created in GEF, with 1 million simulated fission events per reaction. Using the list-mode data feature, the perturbed data were assembled in the TALYS database format and then placed in the database. To enable TALYS to distinguish, and use, the perturbed files in the database, a new keyword was introduced and used to pass along the perturbed file name together with the other input data [26]. As mentioned above, there are two sources of uncertainties for a TMC simulation. The statistical uncertainty goes to zero as $E = (\sqrt{n})^{-1}$, where n is the number of simulations [28], and by performing a large set of independent TMC simulations (10,000), the statistical uncertainty is reduced and potential systematic errors that can originate from potential model defects can be explored.

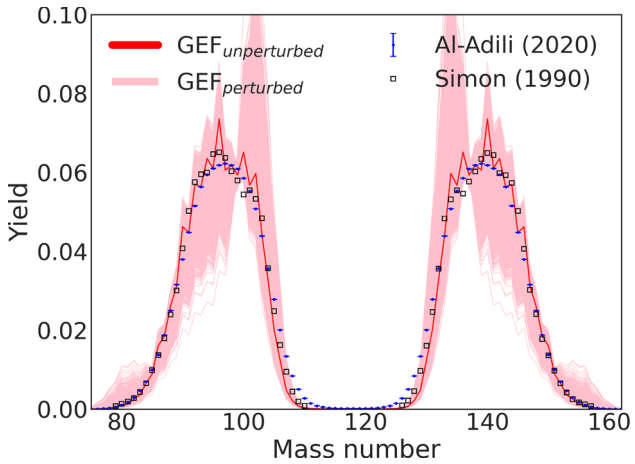

Fig. 1 Calculated pre-neutron emission mass yields from the GEF code for ^{235}U(n$_{th}$,f). The unperturbed default GEF yields are plotted together with 10,000 randomly perturbed yield files, as well as experimental data from Refs. [15,16]

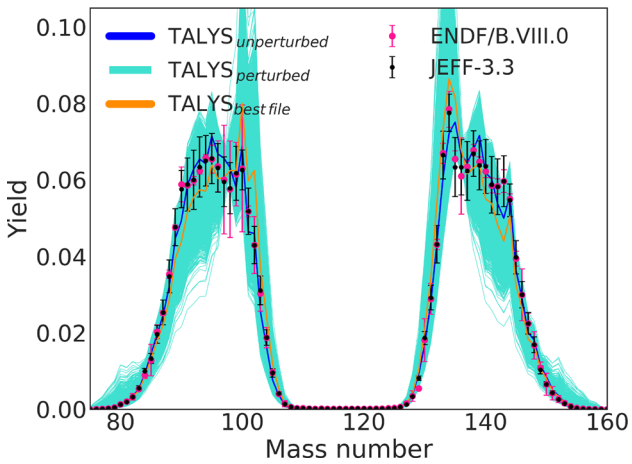

Fig. 2 The post-neutron emission mass yields for ^{235}U(n$_{th}$,f) as calculated by TALYS in comparison to evaluated data from [30,31]. The unperturbed calculation is based on the default GEF input data. The perturbed yields originate from the random GEF yield files

4.2 Random perturbations in GEF

Figure 1 shows the primary fission fragment mass yields as calculated by GEF, in comparison with experimental data from ^{235}U(n$_{th}$,f) [15,16]. The default parameters file is plotted (red solid line) together with the 10,000 random files obtained by perturbing the 94 parameters of GEF (pink solid lines). Upon examination, the distribution of mass yields is strongly correlated to the characteristics of the fission modes. The fluctuations in the calculated yields is prominent around the peak positions of the standard-1, standard-2, and the super-asymmetric fission modes [29]. The yield of the super-long symmetric fission mode seems unaffected, at least as a result of the present parameter variation. Moreover, the magnitude of the yield fluctuations is much larger than the uncertainties of the experimental data, especially in the vicinity of mass numbers 132, 142, and 155. The mean value from all 10,000 random files for the average heavy mass peak position is 140.1, which is fairly close to the value of 140.3 from the default GEF calculation. However, the average heavy mass peaks from the individual random files vary from 139 to 142, with a standard deviation of 0.43 amu. The average total kinetic energy ($\overline{\text{TKE}}$) in the unperturbed GEF calculation is 170.5 MeV. After randomizing the parameters, the $\overline{\text{TKE}}$ exhibits a strong variation with a standard deviation of 1.4 MeV. In addition to the large spread of the values, the average of all $\overline{\text{TKE}}$ values is shifted to 171.0 MeV. This is accompanied by a corresponding change in the average total excitation energy ($\overline{\text{TXE}}$). The unperturbed data show an average value of $\overline{\text{TXE}} \approx 22.6$ MeV. After perturbing the parameters, the values of the $\overline{\text{TXE}}$ are, on average, shifted by roughly 0.2 MeV with a standard deviation of 1.1 MeV.

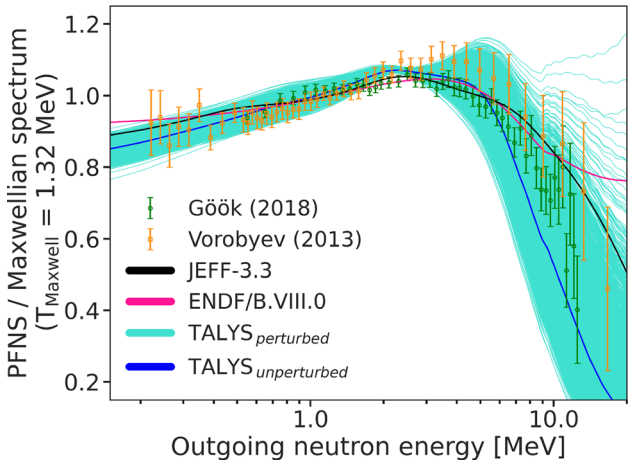

Fig. 3 The prompt fission neutron spectrum (PFNS) from TALYS, using GEF fission yield files as input. The plot shows the calculated ratio to a Maxwell–Boltzmann distribution $\left(f_M = (2\sqrt{E}/(\sqrt{\pi}T^{3/2}))\exp(-\text{E}/\text{T})\right)$, at a temperature of $T = 1.32$ MeV. The default TALYS+GEF is shown together with all random files in comparison with data from Refs. [30–33]

5 Results and Discussion

The proposed methodology of producing random files using GEF and performing the random-file de-excitation using TALYS, was applied to the ^{235}U(n$_{th}$,f) reaction as a proof of principle. Figure 2 displays the fission product yields as determined by TALYS, utilizing both the default GEF input files (represented by a blue solid line) and the 10,000 random GEF files (represented by turquoise solid lines). The distribution of mass yields mirrors the fluctuations observed in the input fission fragment yield data, as illustrated in Fig. 1. Certain areas demonstrate significant variations in yields, while others remain relatively unchanged. As stressed earlier, the

variation in fission product yields is particularly noticeable around the peak positions of the standard-1, standard-2, and super-asymmetric fission modes. Furthermore, the random yield fluctuations are significantly greater than the uncertainties observed in the experimental data, especially for yields around mass numbers 132, 142, and 155.

5.1 Prompt fission neutron emission

Recent studies utilizing the TALYS+GEF framework have found that the prompt fission neutron spectrum (PFNS) may need further improvement through adjustments of the model parameters [2]. A potential source of discrepancy between the calculated PFNS and experimental data could be the input from the default GEF fission databases. Randomly altering the input yield files from GEF has shown potential for refining the TALYS-generated spectrum to align more closely with experimental observations [32], as demonstrated in Fig. 3. This figure shows the ratio of the PFNS distribution to the Maxwell-Boltzmann distribution at a temperature of $T = 1.32$ MeV. The modifications to the PFNS through the use of random GEF files can lead to either an increase or decrease in spectrum hardness. Yet, despite improvements with some of the random files, the spectrum still exhibits discrepancies relative to the experimental data, particularly at higher neutron energies.

The average number of prompt fission neutrons $\overline{\nu}_{\mathrm{n}}(A)$, known to correlate directly with the fragment excitation energy, displays a distinctive saw-tooth pattern and is affected by shell effects. The default average neutron multiplicity from GEF is shown in Fig. 4a, along with the results from 10,000 perturbed GEF de-excitation files. Similarly, Fig. 4b shows the default neutron multiplicity curve from TALYS+GEF, accompanied by the results from 10,000 perturbed TALYS simulations. The data sets agree and indicate notable discrepancies from experimental results [16,32]. In particular, a shift by a few mass units from the experimentally determined minimum around mass 129 can be noticed. Additionally, these results fail to accurately capture the total average neutron emission from heavy and light fragments, with an underestimation of emissions from light fragments and an overestimation from heavy ones. Significant deviations are also observed in the symmetric mass region, hinting to a possible systematic model defect. These discrepancies from recent experimental findings may stem from the assumed excitation energy sharing within the GEF model, affecting the evaporation schemes of both GEF and TALYS+GEF. It is evident from these analyses that a random variation of the parameters with a sigma of 3% from the mean is insufficient to reconcile the discrepancies observed in the neutron emission data.

The average total neutron multiplicity from each random run using GEF and TALYS is depicted in Fig. 5. The default calculations give an average total neutron multiplicity ($\overline{\nu}_{\mathrm{n,tot}}$) of approximately 2.44 for GEF and about 2.41 for TALYS+GEF. The random variations reduced the mean neutron values by 0.04 for GEF and 0.03 for TALYS. In addition, the standard deviation of the neutron multiplicity distribution was 0.16 for the TALYS and 0.15 for GEF. The distribution of average energies per neutron is shown in Fig. 5. GEF gives an average neutron energy around 2.01 MeV, whereas TALYS+GEF gives 1.99 MeV. In contrast to the multiplicity case, the random perturbations have a bigger impact on the standard deviations in GEF compared to TALYS (31 keV in the case of TALYS and 40 keV in the case of GEF).

5.2 Prompt fission γ-ray emission

The emission of γ-rays is another critical component in the de-excitation process of fission products. Once neutron emission has exhausted a major part of the excitation energy, a cascade of γ-rays occurs, which further reduces the excitation energy of the fission products. Figure 6 shows the average γ-ray multiplicity, $\overline{\nu}_{\gamma}(A)$, plotted against the mass of the emitting nucleus, together with experimental data from Ref. [34]. The characteristic saw-tooth pattern of $\overline{\nu}_{\gamma}(A)$ has been reaffirmed by recent investigations [35].

In our work, we verify that TALYS+GEF yields a more distinct saw-tooth pattern, showing better agreement with experimental data compared to the standalone GEF code. GEF has no clear minimum around the doubly magic nucleus at $A = 132$. Applying the 10,000 random variations to both TALYS and GEF does alter the $\overline{\nu}_{\gamma}(A)$ values slightly, but the changes do not improve the overall results. This leads to the conclusion that a 3% random variation in model parameters falls short of solving the observed discrepancies in γ-ray emission characteristics. Moreover, it is doubtful whether a random parameter variation can resolve this issue. It is more likely that a systematic physics-based adjustment is needed for the γ-ray relevant parameters, for instance in the details of the applied level density model or the assumed spin cut-off parameter and the associated fragment moment of inertia. Another potential improvement for fairer comparisons with experimental data is to implement an option to set the γ-ray energy threshold and time coincidence window in the simulations. As highlighted by Talou et al. [36], adjusting the time window can significantly affect the average prompt γ-ray multiplicity and energy due to contributions from long-lived states. Experimental data often employ time coincidence windows that yield a definition of prompt fission γ rays differing from those in theoretical models.

Figure 7 depicts the spread in total average γ-ray multiplicity, following the 10,000 random file calculations. On average, the total γ-ray multiplicity per fission event from GEF is 6.92 and from TALYS it is 7.74. The spread of the total number of γ-rays follows a normal distribution, with a

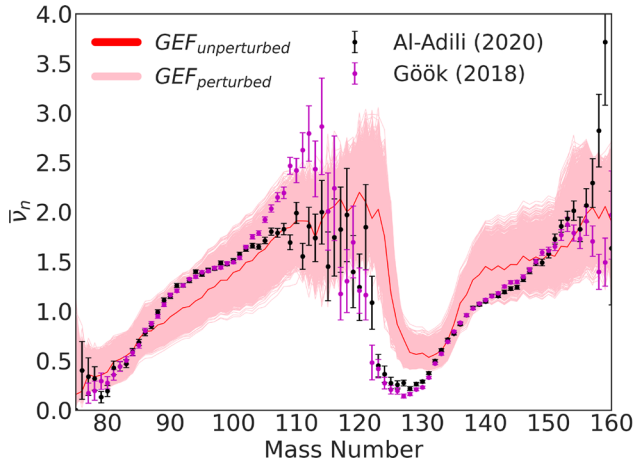

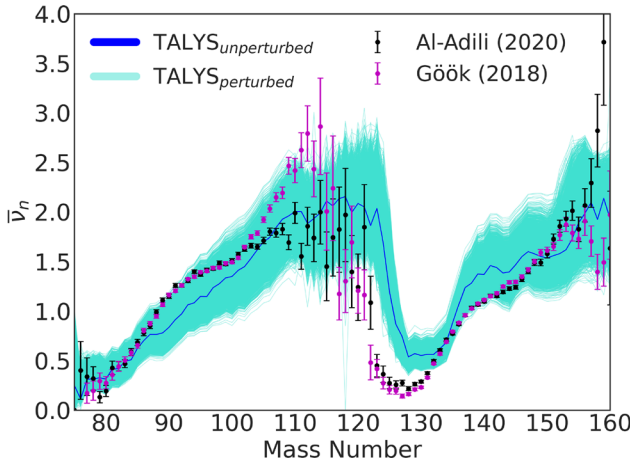

Fig. 4 **a**, Left The average prompt fission neutron multiplicity ($\bar{\nu}_{\mathrm{n}}(A)$) from GEF. The default GEF results are shown together with all random files in comparison with data from Refs. [16,32]. **b**, Right The average prompt fission neutron multiplicity ($\bar{\nu}_{\mathrm{n}}(A)$) from TALYS, using GEF fission yield files as input. The default TALYS+GEF results are shown together with all random files

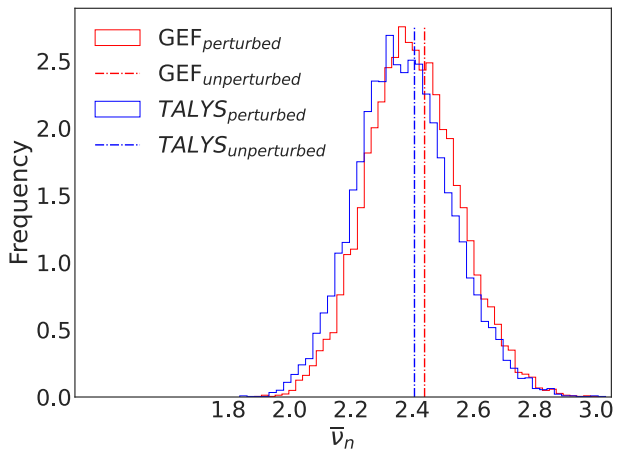

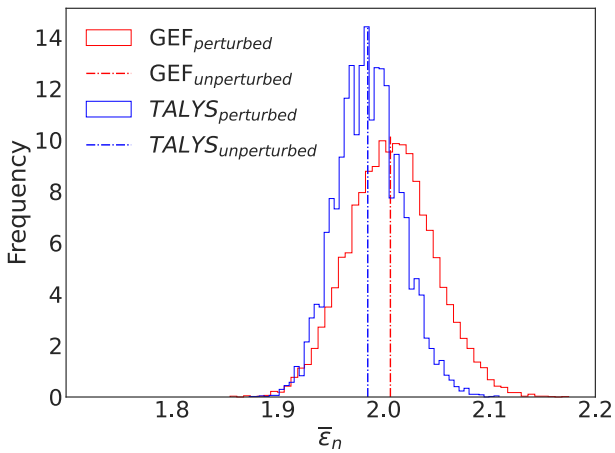

Fig. 5 The distribution of average total prompt fission neutron multiplicity ($\bar{\nu}_{\mathrm{n,tot}}$) from GEF and TALYS+GEF (left). The distribution of average neutron energies per fission neutron ($\bar{\epsilon}_n$) from TALYS, using the random GEF fission yield files as input (right)

standard deviation of 0.11 γ-rays for GEF and 0.10 γ-rays for TALYS. The dashed lines illustrate the calculation using the default input file. In the case of GEF, the random files fluctuate around the default value. However, in the case of TALYS, we observe a shift towards lower mean values of $\bar{\nu}_\gamma\ (A)$ when using the random files.

Figure 7 depicts the average energy of the γ-rays, which is rather different between GEF and TALYS+GEF. The random files introduce a small systematic shift towards higher energy values, compared with the default calculations, which in both cases is below 0.01 MeV. TALYS gives a larger mean value (1.05 MeV/γ) than GEF (0.96 MeV/γ). Integrated over all γ-rays, this amounts to a total difference of about 1.5 MeV. In terms of standard deviation, TALYS exhibits a much larger spread (0.02 MeV) than GEF (0.01 MeV).

5.3 Best-file

One advantage of employing the TMC method lies in its capacity to generate so-called best-files by searching for the parameter set that gives the best agreement with experimental or evaluated data. In this work, we tried to determine the best-file among the limited set of random files for both GEF and TALYS. The best-files were chosen as the file for each code that minimized the relative residuals between the ENDF/B.VIII.0 [30] library values and the calculated values for the average particle multiplicities and energies ($\bar{\nu}_{\mathrm{n}}$, $\bar{\nu}_\gamma$, $\bar{\epsilon}_{\mathrm{n}}$, $\bar{\epsilon}_\gamma$):

$$\text{Best file} \;=\; \min\left(r_{\mathrm{i}}\right), \text{ for } i = 1, 2, ..., 10{,}000,$$

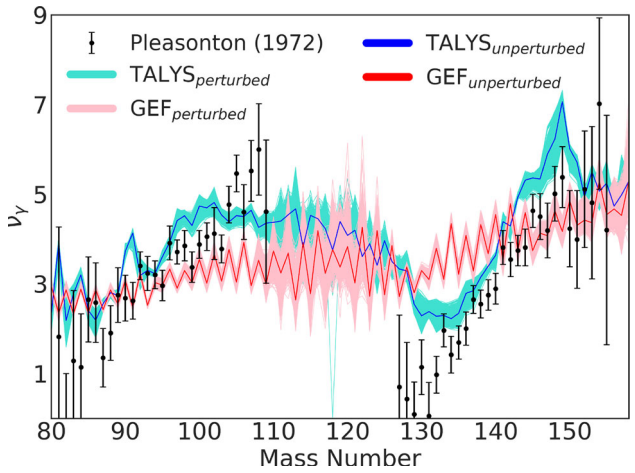

Fig. 6 The average prompt fission γ-ray multiplicity ($\bar{\nu}_\gamma$ (A)) from GEF and TALYS. The default results are shown together with the results from all random files, and in comparison with data from Ref. [34]

where the residual r is given by:

$$r = \sum_{k\,=\,n,\gamma} \left(\left| \frac{\bar{\nu}_\mathrm{k} - \bar{\nu}_\mathrm{k,ENDF}}{\bar{\nu}_\mathrm{k,ENDF}} \right| + \left| \frac{\bar{\epsilon}_\mathrm{k} - \bar{\epsilon}_\mathrm{k,ENDF}}{\bar{\epsilon}_\mathrm{k,ENDF}} \right| \right). \quad (6)$$

As seen in Table 1, the best-files for both GEF and TALYS yield some deviation from the default calculations. The best-file enhances both the GEF and TALYS γ-ray multiplicity results, by virtue of a slightly reduced average total neutron multiplicity and average neutron kinetic energy. Moreover, the average energy of the γ-rays sees a slight improvement in both codes, at the expense of a minor reduction in the average neutron energy.

However, the obtained best-file gives modest enhancements with regard to the ENDF/B.VIII.0 library, at least in the framework of the current random parameter variation. We conclude that a tailored fission model adjustment is needed to further enhance the capability of TALYS to predict fission observables and to construct an improved best-file. Moreover, the best-file determination needs to be reaction- and energy-dependent to accommodate changes in fission characteristics as a function of excitation energy and compound nuclei.

Table 1 Values for selected fission observables (average multiplicities and energies of prompt neutrons and γ rays) from GEF and TALYS, resulting from the file with the smallest overall relative difference compared to ENDF/B.VIII.0 [30]

Simulation	$\bar{\nu}_\mathrm{n}$	$\bar{\epsilon}_\mathrm{n}$ (MeV)	$\bar{\nu}_\gamma$	$\bar{\epsilon}_\gamma$ (MeV)
ENDF/B.VIII.0	2.41	2.00	8.58	0.85
GEF$_{\mathrm{Default}}$	2.44	2.01	6.92	0.95
GEF$_{\mathrm{Best\text{-}file}}$	2.41	1.99	7.18	0.94
TALYS$_{\mathrm{Default}}$	2.41	1.99	7.81	1.05
TALYS$_{\mathrm{Best\text{-}file}}$	2.40	1.97	8.00	1.02

5.4 Angular momentum population

One specific parameter within the GEF model, referred to as J_{scaling}, serves to fine-tune the generation of angular momentum of the primary fission fragments. This parameter acts as a factor to alter the spin cut-off parameter, functioning similarly to the *Rspincutff* keyword in TALYS. In recent studies, angular momentum distributions were modified in TALYS by creating input matrices that externally vary the angular momentum populations [37–39]. The introduction of J_{scaling} within GEF marks a new functionality which enables internal adjustments of angular momentum prior to the TALYS calculations. However, the spin information from GEF is currently not propagated to the TALYS databases. Instead, the

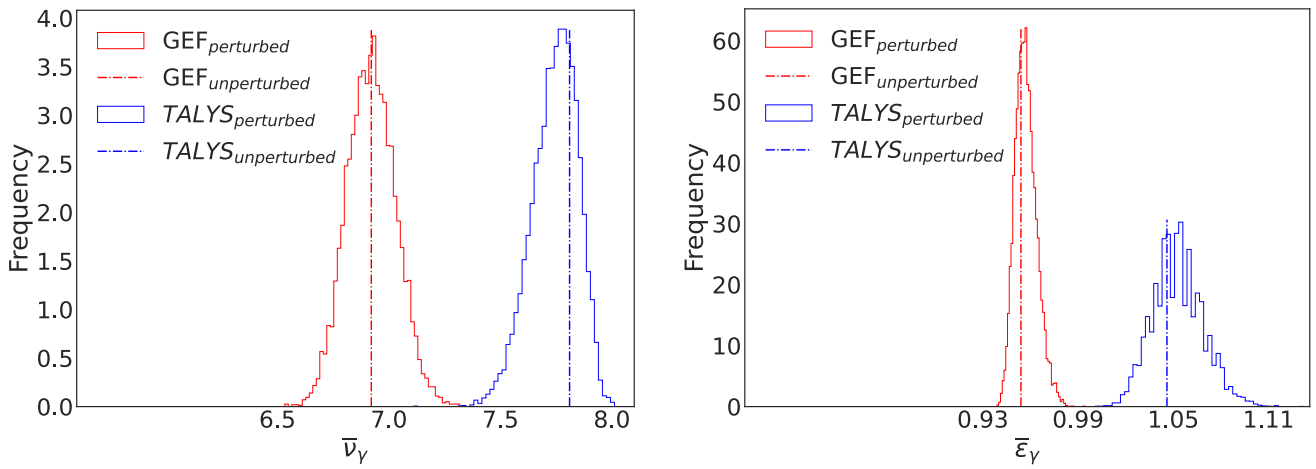

Fig. 7 The average γ-ray multiplicity (left) and average γ-ray energy (right) in the ^{235}U(n$_{\mathrm{th}}$,f) reaction, from the 10,000 random files. The dashed lines indicate the unperturbed values corresponding to the default GEF and TALYS files

angular momentum distributions are produced following the level density formalism using the Rayleigh distribution and the *Rspincutff* parameter (Eq. 5). Here we present a dedicated study to explore the impact of J_{scaling} on the results of GEF and TALYS+GEF. This involved modifying the J_{scaling} and *Rspincutff* parameter values by ±50%, thereby influencing the global population of J in the fission fragments by a substantial amount.

The resulting average prompt evaporation data are presented in Table 2. Changing the J_{scaling} factor from 0.5 to 1.5 in GEF led to an increase of approximately 3 MeV in the average total excitation energy ($\overline{\text{TXE}}$), accompanied by an equal decrease in $\overline{\text{TKE}}$. The increased angular momentum population notably impacted the GEF prompt γ-ray data, where the average γ-ray multiplicity ranged between 5.41 to 8.73, with an average energy difference of 70 keV per γ-ray. Conversely, the average neutron multiplicity remained relatively unchanged, likely due to GEF's assumption that angular momenta are predominantly carried away by E2 γ-rays [27]. Comparing the average number of emitted γ-rays with the evaluated data files may indicate that GEF underestimates the angular momentum population. Similar conclusions were found in earlier studies based on isomeric yield ratios [38].

In the case of TALYS+GEF, employing the default value of *Rspincutff* = 4 while increasing J_{scaling} resulted in a notably higher neutron multiplicity compared to standalone GEF, owing to the increased excitation energy provided to TALYS via the input files from GEF with a higher J_{scaling}. The total neutron multiplicity ($\bar{\nu}_{\text{n,tot}}$) ranged from 2.26 to 2.66. Meanwhile, there was a marginal enhancement in the average total γ-ray multiplicity in proportion to J_{scaling}. The current TALYS database format does not contain information on the angular momentum population from GEF [2]. As a result, the angular momentum in TALYS is not changed when J_{scaling} is changed in GEF, leading to a different correlation between the fragment excitation energies and angular momenta. One potential solution would be to incorporate angular momentum population information into the fission fragment databases, thereby preserving the correlation between fragment excitation energy and rotational energy. As a consequence, TALYS would rely on input data from the fission codes (e.g., GEF) for both nuclide-specific excitation energy and angular momentum.

To mimic a similar scaling of the angular momentum distribution in TALYS, the *Rspincutff* parameter was adjusted from 2 to 6. As seen in Table 2, several notable observations emerge. Firstly, an increase in angular momentum increases $\bar{\nu}_{\text{n,tot}}$ in TALYS, contrary to GEF. Moreover, the neutrons exhibit higher average energies as a function of *Rspincutff*. The emission of γ-rays is significantly impacted in both codes, increasing by approximately 3 γ-rays per fission. The average photon energy decreases by roughly 70 keV for GEF, and 230 keV for TALYS. A higher angular momentum population implies more complex behavior in the prompt evaporation data in TALYS, compared to GEF. This complexity may stem from the prompt fission neutrons, which might carry a substantial part of the angular momentum [8]. Higher neutron energies could imply a higher fraction of partial waves with higher angular momenta removal, according to the optical model [8]. Additionally, differences could emerge from the assumed rigidity of the fission fragments and their respective moment of inertia (Eq. 3). This systematic study clearly indicates a need to adjust both the angular momentum and excitation energy of GEF in order to reproduce the average literature data in TALYS. As a final exercise, we sought to optimize both the J_{scaling} and *Rspincutff* parameters to better match the evaluated average fission data using TALYS+GEF, particularly focusing on the prompt γ-rays. The fine-tuning procedure was conducted separately for the ENDF/B.VIII.0 [30] and JEFF-3.3 [31] libraries. We found that a higher *Rspincutff* parameter value is needed in order to increase the number of γ-rays, as shown in Table 2. In addition, a higher value of the parameter J_{scaling} is required to force a higher average excitation energy. For ENDF/B.VIII.0, the parameters $J_{\text{scaling}} = 1.19$ and *Rspincutff* = 5.38 yielded an excellent match for the evaluated prompt fission neutron data and γ-ray multiplicity, respectively. Similarly, for the JEFF-3.3 library, $J_{\text{scaling}} = 1.22$ and *Rspincutff* = 5.82 provided a good fit. However, in both cases, we were unable to improve the average energy per photon, which is still too large compared to the evaluated data. One possible remedy is to increase the excitation energy histogram spacing, via the *bin* keyword in TALYS. In this work we used a *bin* number of 100 to reduce computational time. It was shown earlier that the average energy per γ-ray decreases as a function of the *bin* number [2].

6 Conclusion and outlook

In this study, we employed the Total Monte Carlo (TMC) approach to evaluate the impact of variations in input data from the GEF code on the evaporation of fission fragments within TALYS. A random variation of the 94 parameters in GEF was introduced following a normal probability distribution with a σ of 3% of the respective parameter value. The parameter variations influenced many aspects of the fission modeling, e.g., the yields of primary fission fragments and their excitation energies. This study focused on the ^{235}U(n_{th},f) reaction, involving the generation of 10,000 random files. Our findings indicate that these changes significantly affect the quantities and energy distributions of both prompt fission neutrons and γ-rays. The developed tool illustrates the applicability of the TMC method for fission calculations and for addressing inaccuracies in model pre-

Table 2 Calculated total average prompt neutron ($\overline{\nu}_n$) and γ-ray ($\overline{\nu}_\gamma$) multiplicities, average particle energies ($\overline{\epsilon}_n$ and $\overline{\epsilon}_\gamma$), for GEF and TALYS, respectively

Code	J_{scaling}	*Rspincutff*	$\overline{\nu}_n$	$\overline{\epsilon}_n$ (MeV)	$\overline{\nu}_\gamma$	$\overline{\epsilon}_\gamma$ (MeV)	$\overline{\text{TXE}}$ (MeV)	$\overline{\text{TKE}}$ (MeV)
GEF	0.50	–	2.45	2.01	5.41	1.00	21.43	171.63
	1.00	–	2.44	2.01	6.92	0.95	22.57	170.47
	1.50	–	2.43	2.00	8.73	0.93	24.44	168.61
TALYS	0.50	4.00	2.26	1.97	7.69	1.04	21.43	171.63
	1.00	4.00	2.41	1.99	7.81	1.05	22.57	170.47
	1.50	4.00	2.66	2.02	7.87	1.06	24.44	168.61
TALYS	0.50	2.00	2.43	1.91	5.66	1.26	21.42	171.64
	1.00	4.00	2.41	1.99	7.81	1.05	22.57	170.47
	1.50	6.00	2.56	2.07	8.68	1.03	24.45	168.62
ENDF/B.VIII.0	–	–	2.41	2.00	8.58	0.85	–	–
$\text{TALYS}_{\text{ENDF}}$	1.19	5.38	2.41	2.03	8.58	1.02	23.19	169.88
JEFF-3.3	–	–	2.41	2.01	8.74	0.81	–	–
$\text{TALYS}_{\text{JEFF}}$	1.22	5.82	2.41	2.05	8.70	1.01	23.31	169.75

Moreover, the average total fragment excitation energy ($\overline{\text{TXE}}$) and total average kinetic energies ($\overline{\text{TKE}}$) are tabulated for each run. The results are based on the adjustment of the parameters J_{scaling} in GEF and *Rspincutff* in TALYS, which govern the angular momenta and the excitation energies of the fission fragments. The default parameter values are $J_{\text{scaling}} = 1.0$ and *Rspincutff* = 4. The last section represents the optimized parameters to reproduce the evaluated neutron and γ-ray data for ENDF/B.VIII.0 [30] and JEFF-3.3 [31], respectively

dictions of fission yields and the energy distribution assumed in nuclear fission processes.

Looking ahead, the isomeric yield ratios (IYRs) also need to be investigated. Extensive attempts have been made to use TALYS for IYR calculations, but most of these efforts treated each precursor in isolation, not considering its relation to other precursors or to the fission partner [37–44]. Very little focus was put on the neutron and γ-ray emissions in these studies. Thus, using this new methodology, one could attempt to optimize the angular momentum population, both to reproduce measured IYR data and to evaluate and correlate prompt neutron and γ-ray data. Moving forward, a refinement to our approach would be a full integration of the angular momentum population, considering complete energy-angular momentum ($E^* - J$) correlations for all fission fragments, including the treatment of orbital angular momentum.

Acknowledgements This work is part of the MÅSTE project (P2023-01281), supported by the Swedish Energy Agency. Additionally, the project contributes to the IAEA Coordinated Research Project on Fission Yields of Actinides (Agreement No. 24005/R0). This work was supported by the Swedish Research Council (VR ref. no. 2019-05385), the Swedish Centre for Nuclear Technology (SKC) and the Swedish Radiation Safety Authority (SSM). A.A. would like to acknowledge Liljewalch travel scholarships and Ingegerd Berghs stiftelse for their research grants. The authors acknowledge Harald och Louise Ekmans forskningsstiftelse for the generous grant at Sigtunastiftelsen.

Funding Open access funding provided by Uppsala University.

Data Availability Statement This manuscript has no associated data or the data will not be deposited. [Author's comment: The datasets are large and cannot be uploaded for practical reasons. But they are available from the authors on reasonable request.]

Code Availability Statement Code/software cannot be made available for reasons disclosed in the code availability statement. [Author's comment: The code is available on Github: https://github.com/UPTEC-F-23065/Modification-of-TALYS-for-TMC-simulations.git, https://github.com/UPTEC-F-23065/McPUFF.git.]

References

1. V. Piau, O. Litaize, A. Chebboubi, S. Oberstedt, A. Göök, A. Oberstedt, Neutron and gamma multiplicities calculated in the consistent framework of the Hauser–Feshbach Monte Carlo code FIFRELIN. Phys. Lett. B **837**, 137648 (2023)
2. K. Fujio, A. Al-Adili, F. Nordström, J.-F. Lemaître, S. Okumura, S. Chiba, A. Koning, Talys calculations of prompt fission observables and independent fission product yields for the neutron-induced fission of ^{235}U. Eur. Phys. J. A **59**(8), 178 (2023)

3. K. Fujio, A. Al-Adili, F. Nordström, J.-F. Lemaître, S. Okumura, S. Chiba, A. Koning Prompt-fission observable and fission yield calculations for actinides by talys. EPJ Web Conf. **292**, 08004 (2024)
4. W. Hauser, H. Feshbach, The inelastic scattering of neutrons. Phys. Rev. **87**, 366–373 (1952)
5. K.-H. Schmidt, B. Jurado, Entropy driven excitation energy sorting in superfluid fission dynamics. Phys. Rev. Lett. **104**, 212501 (2010)
6. F. Nordström. Benchmark of the fission channels in TALYS. Technical Report UPTEC ES 21016. Uppsala university (2021)
7. O. Litaize, O. Serot, L. Berge, Fission modelling with fifrelin. Eur. Phys. J. A **51**(12), 177 (2015)
8. I. Stetcu, A.E. Lovell, P. Talou, T. Kawano, S. Marin, S.A. Pozzi, A. Bulgac, Angular momentum removal by neutron and γ-ray emissions during fission fragment decays. Phys. Rev. Lett. **127**, 222502 (2021)
9. J.N. Wilson, D. Thisse, M. Lebois, N. Jovancevic, D. Gjestvang, R. Canavan, M. Rudigier, D. Étasse, R.-B. Gerst, L. Gaudefroy, E. Adamska, P. Adsley, A. Algora, M. Babo, K. Belvedere, J. Benito, G. Benzoni, A. Blazhev, A. Boso, S. Bottoni, M. Bunce, R. Chakma, N. Cieplicka-Orynczak, S. Courtin, M.L. Cortés, P. Davies, C. Delafosse, M. Fallot, B. Fornal, L. Fraile, A. Gottardo, V. Guadilla, G. Häfner, K. Hauschild, M. Heine, C. Henrich, I. Homm, F. Ibrahim, L.W. Iskra, P. Ivanov, S. Jazrawi, A. Korgul, P. Koseoglou, T. Kröll, T. Kurtukian-Nieto, L. Le Meur, S. Leoni, J. Ljungvall, A. Lopez-Martens, R. Lozeva, I. Matea, K. Miernik, J. Nemer, S. Oberstedt, W. Paulsen, M. Piersa, Y. Popovitch, C. Porzio, L. Qi, D. Ralet, P.H. Regan, K. Rezynkina, V. Sánchez-Tembleque, S. Siem, C. Schmitt, P.-A. Söderström, C. Sürder, G. Tocabens, V. Vedia, D. Verney, N. Warr, B. Wasilewska, J. Wiederhold, M. Yavahchova, F. Zeiser, S. Ziliani, Angular momentum generation in nuclear fission. Nature **590**(7847), 566–570 (2021)
10. J. Randrup, R. Vogt, Generation of fragment angular momentum in fission. Phys. Rev. Lett. **127**, 062502 (2021)
11. A. Bulgac, I. Abdurrahman, S. Jin, K. Godbey, N. Schunck, I. Stetcu, Fission fragment intrinsic spins and their correlations. Phys. Rev. Lett. **126**, 142502 (2021)
12. P. Marević, N. Schunck, J. Randrup, R. Vogt, Angular momentum of fission fragments from microscopic theory. Phys. Rev. C **104**, L021601 (2021)
13. A. Bulgac, I. Abdurrahman, K. Godbey, I. Stetcu, Fragment intrinsic spins and fragments' relative orbital angular momentum in nuclear fission. Phys. Rev. Lett. **128**, 022501 (2022)
14. P. Fong, Statistical theory of nuclear fission: asymmetric fission. Phys. Rev. **102**, 434–448 (1956)
15. G. Simon, J. Trochon, F. Brisard, C. Signarbieux, Pulse height defect in an ionization chamber investigated by cold fission measurements. Nucl. Instrum. Methods Phys. Res. Sect. A Accel. Spectrom. Detect. Assoc. Equip. **286**(1), 220–229 (1990)
16. A. Al-Adili, D. Tarrío, K. Jansson, V. Rakopoulos, A. Solders, S. Pomp, A. Göök, F.-J. Hambsch, S. Oberstedt, M. Vidali, Prompt fission neutron yields in thermal fission of ^{235}U and spontaneous fission of ^{252}Cf. Phys. Rev. C **102**, 064610 (2020)
17. N. Feather, Emission of neutrons from moving fission fragments. Technical Report BM-148, British Mission (1942)
18. H.A. Bethe, An attempt to calculate the number of energy levels of a heavy nucleus. Phys. Rev. **50**, 332–341 (1936)
19. S. Okumura, T. Kawano, P. Jaffke, P. Talou, S. Chiba, ^{235}U(n, f) independent fission product yield and isomeric ratio calculated with the statistical Hauser–Feshbach theory. J. Nucl. Sci. Technol. **55**(9), 1009–1023 (2018)
20. S. Cannarozzo, S. Pomp, A. Solders, A. Al-Adili, A. Göök, A. Koning, Global comparison between experimentally measured isomeric yield ratios and nuclear model calculations. Eur. Phys. J. A **59**(12), 295 (2023)
21. A. Rodrigo, N. Otuka, S. Takács, A.J. Koning, Compilation of isomeric ratios of light particle induced nuclear reactions. At. Data Nucl. Data Tables **153**, 101583 (2023)
22. A.J. Koning, D. Rochman, Towards sustainable nuclear energy: putting nuclear physics to work. Ann. Nucl. Energy **35**(11), 2024–2030 (2008)
23. A.J. Koning, D. Rochman, Modern nuclear data evaluation with the TALYS code system. Nucl. Data Sheets **113**(12), 2841–2934 (2012)
24. D. Rochman, S.C. van der Marck, A.J. Koning, H. Sjöstrand, W. Zwermann, Uncertainty propagation with fast Monte Carlo techniques. Nucl. Data Sheets **118**, 367–369 (2014)
25. D. Rochman, A.J. Koning, S.C. van der Marck, A. Hogenbirk, C.M. Sciolla, Nuclear data uncertainty propagation: perturbation vs. Monte Carlo. Ann. Nucl. Energy **38**(5), 942–952 (2011)
26. P. Karlsson. Total Monte Carlo of the fission model in GEF and its influence on the nuclear evaporation in TALYS. Technical Report UPTEC F 23065, Uppsala university (2023)
27. K.-H. Schmidt, B. Jurado, C. Amouroux, C. Schmitt, General description of fission observables: GEF model code. Nucl. Data Sheets **131**, 107–221 (2016)
28. T. Michael, *Heath, Scientific Computing: An Introductory Survey*, 2nd edn. (McGraw-Hill, Boston, 2005)
29. U. Brosa, S. Grossmann, A. Muller, Nuclear scission. Phys. Rep. **197**(4), 167–262 (1990)
30. D.A. Brown, M.B. Chadwick, R. Capote, A.C. Kahler, A. Trkov, M.W. Herman, A.A. Sonzogni, Y. Danon, A.D. Carlson, M. Dunn, D.L. Smith, G.M. Hale, G. Arbanas, R. Arcilla, C.R. Bates, B. Beck, B. Becker, F. Brown, R.J. Casperson, J. Conlin, D.E. Cullen, M.A. Descalle, R. Firestone, T. Gaines, K.H. Guber, A.I. Hawari, J. Holmes, T.D. Johnson, T. Kawano, B.C. Kiedrowski, A.J. Koning, S. Kopecky, L. Leal, J.P. Lestone, C. Lubitz, J.I. Márquez Damián, C.M. Mattoon, E.A. McCutchan, S. Mughabghab, P. Navratil, D. Neudecker, G.P.A. Nobre, G. Noguere, M. Paris, M. T. Pigni, A.J. Plompen, B. Pritychenko, V.G. Pronyaev, D. Roubtsov, D. Rochman, P. Romano, P. Schillebeeckx, S. Simakov, M. Sin, I. Sirakov, B. Sleaford, V. Sobes, E.S. Soukhovitskii, I. Stetcu, P. Talou, I. Thompson, S. van der Marck, L. Welser-Sherrill, D. Wiarda, M. White, J.L. Wormald, R.Q. Wright, M. Zerkle, G. Žerovnik, Y. Zhu, ENDF/B-VIII.0: The 8th Major Release of the Nuclear Reaction Data Library with CIELO-project Cross Sections, New Standards and Thermal Scattering Data. Nucl. Data Sheets **148**, 1–142 (2018)
31. A.J.M. Plompen, O. Cabellos, C. De Saint Jean, M. Fleming, A. Algora, M. Angelone, P. Archier, E. Bauge, O. Bersillon, A. Blokhin, F. Cantargi, A. Chebboubi, C. Diez, H. Duarte, E. Dupont, J. Dyrda, B. Erasmus, L. Fiorito, U. Fischer, D. Flammini, D. Foligno, M.R. Gilbert, J.R. Granada, W. Haeck, F.J. Hambsch, P. Helgesson, S. Hilaire, I. Hill, M. Hursin, R. Ichou, R. Jacqmin, B. Jansky, C. Jouanne, M.A. Kellett, D.H. Kim, H.I. Kim, I. Kodeli, A.J. Koning, A.Y. Konobeyev, S. Kopecky, B. Kos, A. Krása, L.C. Leal, N. Leclaire, P. Leconte, Y.O. Lee, H. Leeb, O. Litaize, M. Majerle, J.I. Márquez Damián, F. Michel-Sendis, R.W. Mills, B. Morillon, G. Noguère, M. Pecchia, S. Pelloni, P. Pereslavtsev, R.J. Perry, D. Rochman, A. Röhrmoser, P. Romain, P. Romojaro, D. Roubtsov, P. Sauvan, P. Schillebeeckx, K.H. Schmidt, O. Serot, S. Simakov, I. Sirakov, H. Sjöstrand, A. Stankovskiy, J.C. Sublet, P. Tamagno, A. Trkov, S. van der Marck, F. Álvarez-Velarde, R. Villari, T.C. Ware, K. Yokoyama, G. Žerovnik. The joint evaluated fission and fusion nuclear data library, JEFF-3.3. Eur. Phys. J. A, **56**(7), 181 (2020)
32. A. Göök, F.-J. Hambsch, S. Oberstedt, M. Vidali, Prompt neutrons in correlation with fission fragments from ^{235}U(n, f). Phys. Rev. C **98**, 044615 (2018)
33. A.S. Vorobyev, O.A. Shcherbakov, Integral prompt neutron spectrum for fission of 235u by thermal neutrons. *(J,YK,,(1-2),37,2013)*

Jour: Vop.At.Nauki i Tekhn.,Ser.Yaderno-Reak.Konstanty., 1-2:37, 2013. English translation published as report: USSR report to the I.N.D.C., No.0455, p.21 (2014), Austria, EXFOR entry: 41597
34. F. Pleasonton, R.L. Ferguson, H.W. Schmitt, Prompt gamma rays emitted in the thermal-neutron-induced fission of ^{235}U. Phys. Rev. C **6**, 1023–1039 (1972)
35. M. Travar, V. Piau, A. Göök, O. Litaize, J. Nikolov, A. Oberstedt, S. Oberstedt, J. Enders, M. Peck, W. Geerts, M. Vidali, Experimental information on mass- and TKE-dependence of the prompt fission γ-ray multiplicity. Phys. Lett. B **817**, 136293 (2021)
36. P. Talou, T. Kawano, I. Stetcu, J.P. Lestone, E. McKigney, M.B. Chadwick, Late-time emission of prompt fission γ rays. Phys. Rev. C **94**(6), (2016)
37. A. Al-Adili, V. Rakopoulos, A. Solders, Extraction of angular momenta from isomeric yield ratios—employing talys to de-excite primary fission fragments. Eur. Phys. J. A **55**(4), 61 (2019)
38. A. Al-Adili, A. Solders, V. Rakopoulos, Employing talys to deduce angular momentum root mean-square values, Jrms, in fission fragments. EPJ Web Conf. **239**, 03019 (2020)
39. Z. Gao, A. Solders, A. Al-Adili, S. Cannarozzo, M. Lantz, S. Pomp, H. Sjöstrand, Estimating angular momenta of fission fragments from isomeric yield ratios using talys. Phys. Rev. C **109**, 064626 (2024)
40. D. Gjestvang, J.N. Wilson, A. Al-Adili, S. Siem, Z. Gao, J. Randrup, D. Thisse, M. Lebois, N. Jovančević, R. Canavan, M. Rudigier, D. Étasse, R.-B. Gerst, E. Adamska, P. Adsley, A. Algora, C. Belvedere, J. Benito, G. Benzoni, A. Blazhev, A. Boso, S. Bottoni, M. Bunce, R. Chakma, N. Cieplicka-Oryńczak, S. Courtin, M.L. Cortés, P. Davies, C. Delafosse, M. Fallot, B. Fornal, L. Fraile, A. Gottardo, V. Guadilla, G. Häfner, K. Hauschild, M. Heine, C. Henrich, I. Homm, F. Ibrahim, ŁW. Iskra, P. Ivanov, S. Jazrawi, A. Korgul, P. Koseoglou, T. Kröll, T. Kurtukian-Nieto, S. Leoni, J. Ljungvall, A. Lopez-Martens, R. Lozeva, I. Matea, K. Miernik, J. Nemer, S. Oberstedt, W. Paulsen, M. Piersa-Siłkowska, Y. Popovitch, C. Porzio, L. Qi, P.H. Regan, K. Rezynkina, V. Sánchez-Tembleque, C. Schmitt, P.-A. Söderström, C. Sürder, G. Tocabens, V. Vedia, D. Verney, N. Warr, B. Wasilewska, J. Wiederhold, M. Yavahchova, S. Ziliani, Examination of how properties of a fissioning system impact isomeric yield ratios of the fragments. Phys. Rev. C **108**, 064602 (2023)
41. Z. Gao, A. Solders, A. Al-Adili, S. Cannarozzo, M. Lantz, S. Pomp, O. Beliuskina, T. Eronen, S. Geldhof, A. Kankainen, I.D. Moore, D. Nesterenko, H. Penttilä, Isomeric yield ratios in proton-induced fission of ^{238}U. Phys. Rev. C **108**, 054613 (2023)
42. A. Al-Adili, Z. Gao, M. Lantz, A. Solders, M. Österlund, S. Pomp, Isomer yields in nuclear fission. EPJ Web Conf. **256**, 00002 (2021)
43. V. Rakopoulos, M. Lantz, S. Pomp, A. Solders, A. Al-Adili, L. Canete, T. Eronen, A. Jokinen, A. Kankainen, A. Mattera, I.D. Moore, D.A. Nesterenko, M. Reponen, S. Rinta-Antila, A. de Roubin, M. Vilén, M. Österlund, H. Penttilä, Isomeric fission yield ratios for odd-mass cd and in isotopes using the phase-imaging ion-cyclotron-resonance technique. Phys. Rev. C **99**, 014617 (2019)
44. V. Rakopoulos, M. Lantz, A. Solders, A. Al-Adili, A. Mattera, L. Canete, T. Eronen, D. Gorelov, A. Jokinen, A. Kankainen, V.S. Kolhinen, I.D. Moore, D.A. Nesterenko, H. Penttilä, I. Pohjalainen, S. Rinta-Antila, V. Simutkin, M. Vilén, A. Voss, S. Pomp, First isomeric yield ratio measurements by direct ion counting and implications for the angular momentum of the primary fission fragments. Phys. Rev. C **98**, 024612 (2018)